NASA CONTRACTOR REPORT

NASA CR-192(01)

DERIVATION OF MAPPING FUNCTIONS FOR STAR-SHAPED REGIONS

SUPPLEMENT

by Kwan Rim and Roger O. Stafford

Prepared under Grant No. NsG-576 *by*
UNIVERSITY OF IOWA
Iowa City, Iowa
for

NATIONAL AERONAUTICS AND SPACE ADMINISTRATION • WASHINGTON, D. C. • APRIL 1966

DERIVATION OF MAPPING FUNCTIONS FOR STAR-SHAPED REGIONS

SUPPLEMENT

By Kwan Rim and Roger O. Stafford

Prepared under Grant No. NsG-576 by
UNIVERSITY OF IOWA
Iowa City, Iowa

for

NATIONAL AERONAUTICS AND SPACE ADMINISTRATION

For sale by the Clearinghouse for Federal Scientific and Technical Information
Springfield, Virginia 22151 – Price $0.45

ABSTRACT

SUPPLEMENT TO NASA CR-192

DERIVATION OF MAPPING FUNCTIONS FOR STAR-SHAPED REGIONS

This report presents an extension of the method derived in NASA CR-192 to the problem of interior-to-interior mapping by the Schwarz-Christoffel transformation. The information presented herein is restricted to the same class of star-shaped regions analyzed in NASA CR-192, although the method of analysis can be readily extended to problems with any polygonal boundary.

This supplement and its original report, NASA CR-192, constitute a complete report on the derivation of mapping functions for a large class of star-shaped regions by means of the Schwarz-Christoffel transformation.

TABLE OF CONTENTS

SECTIONS	PAGE
SUMMARY	1
INTRODUCTION	1
DERIVATION OF EQUATIONS	2
PARAMETERS CONTROLLING SIZE AND SHAPE	4
EFFECT OF TRUNCATION	5
CONSTRUCTION OF MAPPING FUNCTIONS	6
CONCLUDING REMARKS	6
APPENDIX S-A Analysis of Second-Degree Stars	8
APPENDIX S-B Examples of Mapped Stars	19
APPENDIX S-C Computer Programs	21

SUPPLEMENT TO NASA CR-192;

DERIVATION OF MAPPING FUNCTIONS FOR STAR-SHAPED REGIONS

By Kwan Rim and Roger O. Stafford

Department of Mechanics and Hydraulics
The University of Iowa
Iowa City, Iowa

SUMMARY

In the previous report on mapping functions, NASA CR-192, March, 1965, a general method based on the Schwarz-Christoffel transformation was developed for mapping the exterior of a unit circle onto the exterior of a star-shaped polygon. The present report is an extension of the previous work to include the mapping of the interior of a unit circle onto the interior of a star-shaped polygon.

INTRODUCTION

The purpose of the main report (NASA CR-192) was to present a simple method of deriving the approximate mapping functions in the form of low-order polynomials, which transacted the conformal mapping of the exterior of a unit circle onto the exterior of a star-shaped polygon. The derivation was based on the well-known Schwarz-Christoffel transformation.

Now, an almost identical method has been developed for mapping the interior of a unit circle onto the interior of a star-shaped polygon. This method leads to equations which are identical in form to those derived in NASA CR-192. Thus, most of the techniques of application and remarks set forth in the original report apply directly to the conformal transformation of interior regions. In fact, practically the same algorithm can be used to transact either exterior-to-exterior or interior-to-interior mappings.

The generality can be further extended to include the mapping of either the interior or the exterior of a unit circle onto either the exterior or the interior of a star-shaped polygon, through the simple substitution of $\zeta = 1/\bar{\zeta}$. Therefore, we have developed one simple technique which would handle various types of transformations of star-shaped polygons. In terms of physical problems, this provides a means of solving solid propellent rocket motors, gears, interior and exterior splined shafts, etc.

Because of the great similarity in the derivations, many of the details given in the original report will not be duplicated here. For the definitions of symbols and conventions, references, and equation and figure numbers, refer to NASA CR-192. The equation and figure numbers used in the Supplement have the prefix S if they first appear here, otherwise they are the same equation numbers as are given in the original report.

DERIVATION OF EQUATIONS

The conformal mapping of the interior of a unit circle onto the interior of a closed polygon is accomplished by the application of the Schwarz-Christoffel transformation:

$$z = f(\zeta) = A \int_0^{\zeta} (\zeta_1 - \zeta)^{-K_1} (\zeta_2 - \zeta)^{-K_2} \cdots (\zeta_m - \zeta)^{-K_m} d\zeta \qquad \text{(S-1)}$$

in which πK_j is the exterior angle of the polygon at the vertex z_j, and ζ_j is the image of the j-th vertex on the unit circle. Refer to figure 1 for other details.

Consider the group of geometric shapes that may be well approximated by the type of polygon shown in figure 2. The mapping function for this kind of polygon is sufficiently simple so as to facilitate a lucid derivation, yet it retains those details which allow an easy generalization to an arbitrary star.

Proper substitution and regrouping of terms in equation (S-1) reduces the mapping function to

$$z = A \int_0^{\zeta} \frac{[(d_1 - \zeta)\ldots(d_m - \zeta)]^{K_3} \cdot [(c_1 - \zeta) \ldots(c_m - \zeta)]^{K_2}}{[(a_1 - \zeta)\ldots(a_m - \zeta)]^{K_0} \cdot [(b_1 - \zeta) \ldots(b_m - \zeta)]^{K_1}}$$

$$\times \frac{[(e_1 - \zeta)\ldots(e_m - \zeta)]^{K_2}}{[(f_1 - \zeta)\ldots(f_m - \zeta)]^{K_1}} d\zeta \qquad \text{(S-2)}$$

in which a_j, b_j, ... f_j are defined by

$$a_1 = e^{i \cdot 0}, \; b_1 = e^{i\gamma_1}, \; c_1 = e^{i\gamma_2}, \; d_1 = e^{i\frac{\pi}{m}}, \; e_1 = e^{i(\frac{2\pi}{m} - \gamma_2)}, \; f_1 = e^{i(\frac{2\pi}{m} - \gamma_1)},$$

and by the general relationship

$$\beta_j \equiv \beta_1 \cdot e^{i\frac{2\pi}{m}(j-1)} \; ; \quad \beta_j = a_j, b_j, \ldots f_j; \quad (j = 1, 2, \ldots m).$$

It can be shown that

$$(\beta_1 - \zeta)(\beta_2 - \zeta) \ldots (\beta_m - \zeta) = \prod_{j=1}^{m} [\beta_1 e^{i\frac{2\pi}{m}(j-1)} - \zeta] = \beta_1^m - \zeta^m.$$

Since a_m and d_m are the m-th roots of +1 and -1 respectively, the mapping function reduces to

$$z = A \int_0^{\zeta} \frac{(1 + \zeta^m)^{K_3} \cdot [(1 - e^{-im\gamma_2}\zeta^m)(1 - e^{im\gamma_2}\zeta^m)]^{K_2}}{(1 - \zeta^m)^{K_0} \cdot [(1 - e^{-im\gamma_1}\zeta^m)(1 - e^{im\gamma_1}\zeta^m)]^{K_1}} d\zeta. \qquad \text{(S-3)}$$

The integral in equation (S-2) is evaluated by expanding the integrand in a power series and integrating it term by term. To do so, a general series associated with the j-th vertex is first developed, then the integrand is formed from the product of these series. The terms associated with the j-th vertex can be written as

$$[(1 - e^{-im\gamma_j}\zeta^m)(1 - e^{im\gamma_j}\zeta^m)]^{K_j} = \sum_{k=0}^{\infty} C_k (\gamma_j, K_j) \cdot \zeta^{km} = F(\zeta, \gamma_j, K_j), \qquad \text{(S-4)}$$

which is identical to equation (4). The terms associated with the first and last vertices may be regarded as special cases of equation (S-4), as they may be written as

$$(1 - \zeta^m)^{-K_0} = F(\zeta, 0, -\frac{K_0}{2}),$$

$$(1 + \zeta^m)^{K_3} = F(\zeta, \frac{\pi}{m}, \frac{K_3}{2}).$$

Thus equation (S-3) may be expressed as the product of (n + 2) series's defined by equation (S-4):

$$z = \alpha' \int_0^{\zeta} F(\zeta, 0, -\frac{K_0}{2}) \cdot [\prod_{j=1}^{n} F(\zeta, \gamma_j, -K_j)] \cdot F(\zeta, \frac{\pi}{m}, -\frac{K_{n+1}}{2})\, d\zeta, \qquad \text{(S-5)}$$

$$z = \alpha' \int_0^{\zeta} \sum_{k=0}^{\infty} D_k \zeta^{km}\, d\zeta, \qquad \text{(S-6)}$$

where n is the degree of the star-shaped polygon, i.e., the number of vertices between two adjacent lines of symmetry. Thus the mapping function is finally given by

$$z = f(\zeta) = \alpha \sum_{k=0}^{\infty} \frac{D_k}{1 + km} \zeta^{1+km}, \qquad \text{(S-7)}$$

where α is the normalizing coefficient. As expected, equation (S-5) for the mapping of interior domains is identical to the corresponding equation for exterior domains, equation (5), except the signs of K_j are reversed.

The polynomial mapping function for a simply-connected star may also be used for the mapping of a certain doubly-connected star since the function

$$z = f(\zeta) = \sum_{k=0}^{\infty} E_k \zeta^{1+km}$$

reduces to the following equation for $\zeta << 1$;

$$z = f(\zeta) \doteq E_0 \cdot \zeta. \qquad \text{(S-8)}$$

Hence a circle of radius $|\zeta| << 1$ will map onto an approximate circle in the z-plane. In most cases the image of $|\zeta| = 0.5$ will vary from a circle by not more than 4%.

The method presented in NASA CR-192 and in this Supplement may be readily extended to the derivation of a wider class of mapping functions by performing an additional linear fractional transformation on ζ. A linear fractional transformation is of the following form:

$$\zeta = \frac{aw + b}{cw + d}, \quad ad - bc \neq 0.$$

For example, substitution of $\zeta = 1/\overline{w}$ ($\overline{w}$ is the complex conjugate of w) into

$$z = \sum_{k=0}^{\infty} E_k \zeta^{1\pm km}$$

will transact the mapping of the exterior of the unit circle on w-plane onto the interior of the star-shaped polygon when the exponent is $(1 + km)$, and the interior of the unit circle onto the exterior of the star-shaped polygon with the exponent $(1 - km)$.

PARAMETERS CONTROLLING SIZE AND SHAPE

The behavior of the mapping function is controlled by three types of parameters. They are the normalizing coefficient α, the vertex angles (k_1 and k_2) and the spacing of the vertex images (γ_1 and γ_2) on the unit circle. Qualitatively, these parameters control the congruency of an interior-to-interior mapping in exactly the same manner as they did in the case of exterior-to exterior mapping. Therefore the discussion given in NASA CR-192 under the section entitled "Parameters Controlling Size and Shape" will not be repeated here.

In the quantitative sense, however, the relationship between S_k and γ_j for interior-to-interior mapping is considerably different from that for

exterior-to-exterior mapping. Hence a new set of graphical relations of S versus γ for the interior-to-interior mapping of second-degree stars is presented in Appendix S-A.

EFFECT OF TRUNCATION

The determination of the effects of truncation on interior mapping functions is accomplished in exactly the same way that exterior mapping functions are analyzed. Hence Remark I applies directly to interior mapping functions and is repeated here for clarity:

Remark I: Mapping in the vicinity of the j-th vertex is primarily controlled by the j-th binomial; hence the accuracy of the mapping function in that vicinity depends on the accuracy (the extent of truncation) of the corresponding polynomial, e.g., equation (4) or (S-4).

In the case of interior-to-interior mapping, however, the convergence characteristics of the polynomial for a vertex are considerably different from the corresponding case of exterior-to-exterior mapping. An inspection of the typical series for positive and negative vertex angles for each case will clearly delineate the differences. For exterior-to-exterior mapping:

$$\pi K > 0;\ (1 - \zeta)^{K} = 1 - K\zeta + \frac{K(K-1)}{2!}\zeta^2 - \frac{K(K-1)(K-2)}{3!}\zeta^3 + \ldots \qquad \text{(S-9)}$$

$$\pi K < 0;\ (1 + \zeta)^{-K} = 1 - K\zeta + \frac{K(K+1)}{2!}\zeta^2 - \frac{K(K+1)(K+2)}{3!}\zeta^3 + \ldots . \qquad \text{(S-10)}$$

For interior-to-interior mapping:

$$\pi K > 0;\ (1 - \zeta)^{-K} = 1 + K\zeta + \frac{K(K+1)}{2!}\zeta^2 + \frac{K(K+1)(K+2)}{3!}\zeta^3 + \ldots \qquad \text{(S-11)}$$

$$\pi K < 0;\ (1 + \zeta)^{-K} = 1 + K\zeta + \frac{K(K-1)}{2!}\zeta^2 + \frac{K(K-1)(K-2)}{3!}\zeta^3 + \ldots . \qquad \text{(S-12)}$$

The ratio of successive terms for each series is given by

$$R_n^{+} = \frac{n - K}{n + 1} \begin{pmatrix} \text{for positive vertex angles in exterior-to-exterior mapping} \\ \text{for negative vertex angles in interior-to-interior mapping} \end{pmatrix}$$

$$R_n^{-} = \frac{n + K}{n + 1} \begin{pmatrix} \text{for negative vertex angles in exterior-to-exterior mapping} \\ \text{for positive vertex angles in interior-to-interior mapping} \end{pmatrix}.$$

This ratio is a measure of the rate of convergence and we conclude from

$$R_n^{+} < R_n^{-}$$

that series (S-9) or (11) and (S-12) converge faster than series (S-10) or (12) and (S-11). Hence the following remark is in order for interior-to-interior mapping:

Remark II: For the same accuracy of mapping, the polynomial for a vertex with a positive exterior angle requires a greater number of terms than the polynomial for a vertex with a negative exterior angle.

It should also be noted that exterior-to-exterior mapping yields series with alternating signs, while the equivalent series for interior-to-interior mapping has the same sign throughout. Hence, in order to maintain the same level of accuracy, one has to retain more terms in the polynomial mapping function for interior-to-interior mapping than for the corresponding exterior-to-exterior mapping.

CONSTRUCTION OF MAPPING FUNCTIONS

The construction of mapping functions for interior-to-interior mapping from the known data (K_j and S_j) can proceed in exactly the same manner as for exterior-to-exterior mapping. Therefore, the five steps set forth in NASA CR-192 will not be duplicated here. Note that one must use the plots in Appendix S-A to determine the image spacings.

CONCLUDING REMARKS

The methods presented in NASA CR-192, March, 1965, and this Supplement may be considered to be a complete generalization of the application of the Schwarz-Christoffel transformation to the mapping of star-shaped domains.

The advantages and disadvantages of the use of the Schwarz-Christoffel transformation were set forth in the "Concluding Remarks" of NASA CR-192. Since those remarks also apply to interior-to-interior mapping, they will not be recapitulated here. However, some perspective can be gained by the comparison of the two cases.

In the case of exterior-to-exterior mapping, the coefficients of the series for a vertex will have alternating signs; namely the series will be absolutely convergent. Now, in the case of interior-to-interior mapping, the corresponding series does converge but not absolutely. Therefore, the mapping function for interior-to-interior mapping would be more slowly convergent than that for exterior-to-exterior mapping.

In the case of interior-to-interior mapping, it is evident from Remark II that the re-entrant corners of a polygon can be rather accurately mapped, while the vertices with positive exterior angles are usually rounded. Exactly the converse was true in the case of exterior-to-exterior mapping.

In practice this rounding of certain vertices does not significantly affect the accuracy of analytic solutions. For instance, the critical stress concentrations in elasticity problems occur almost always on the boundary of more accurately mapped corners for both the interior and exterior problems. A similar statement is also true in the case of heat conduction problems.

APPENDIX S-A. ANALYSIS OF SECOND-DEGREE STARS

A detailed analysis was performed on a second-degree star with $K_0 = K_3 = 0$. It is similar to what was described in Appendix A of the original report (NASA CR-192). Presented herein is an equivalent set of plots of S_k versus γ_k for interior-to-interior mapping. Even though the plots of S versus γ for interior-to-interior mapping are quite different from those for exterior-to-exterior mapping, the same procedure can be used to determine γ_1 and γ_2 from the given data m, K_1, S_1 and S_2.

The truncation limits for interior mapping functions can be obtained directly from table 1 of NASA CR-192. The speed of convergence of an interior mapping function at a vertex with a positive angle is nearly equal to that of an exterior mapping function at a vertex with a negative angle. Hence it has been found that the number of terms required for S_1 in an interior mapping function is equal to about 1.5 times what was required for S_2 in an exterior-to-exterior mapping function. A similar relation holds between S_2 in interior-to-interior mapping and S_1 in exterior-to-exterior mapping. The approximate factor of 1.5 is due to the fact that interior mapping functions always converge more slowly than exterior mapping functions.

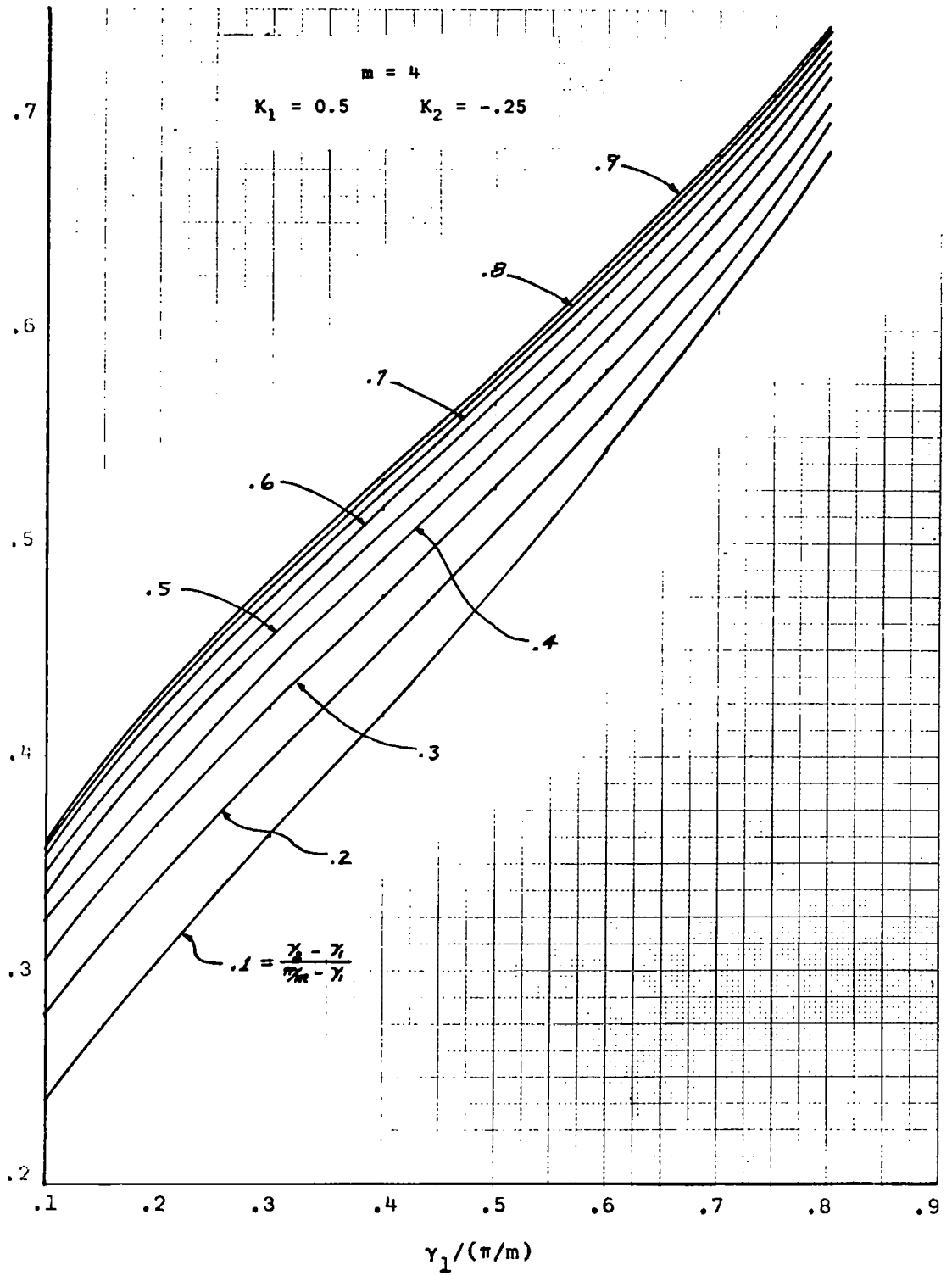

Figure S-1.- S_1 Versus $\gamma_1/(\pi/m)$ for $(\gamma_2 - \gamma_1)/(\pi/m - \gamma_1)$ = constant.

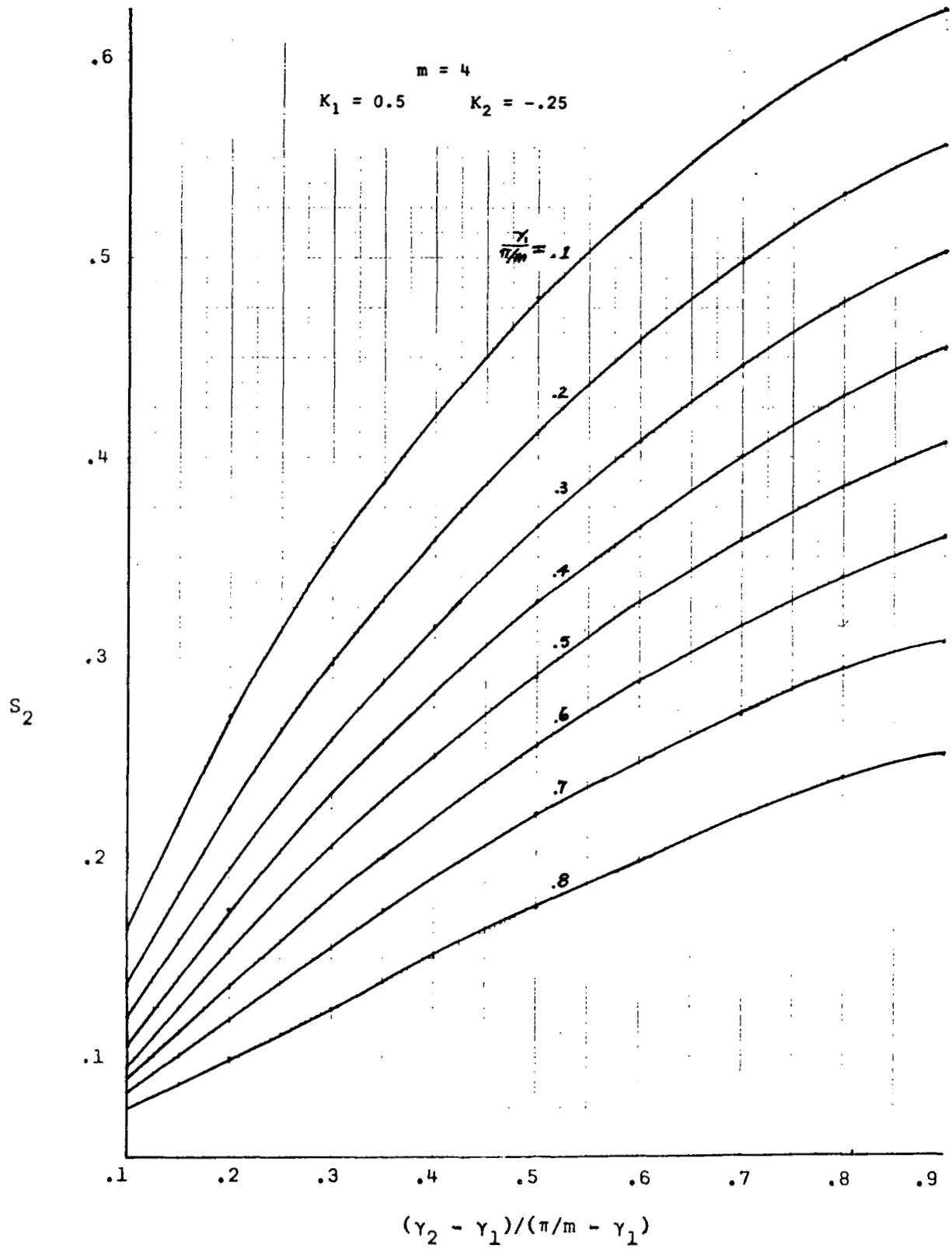

Figure S-2.- S_2 versus $(\gamma_2 - \gamma_1)/(\pi/m - \gamma_1)$ for $\gamma_1/(\pi/m)$ = constant.

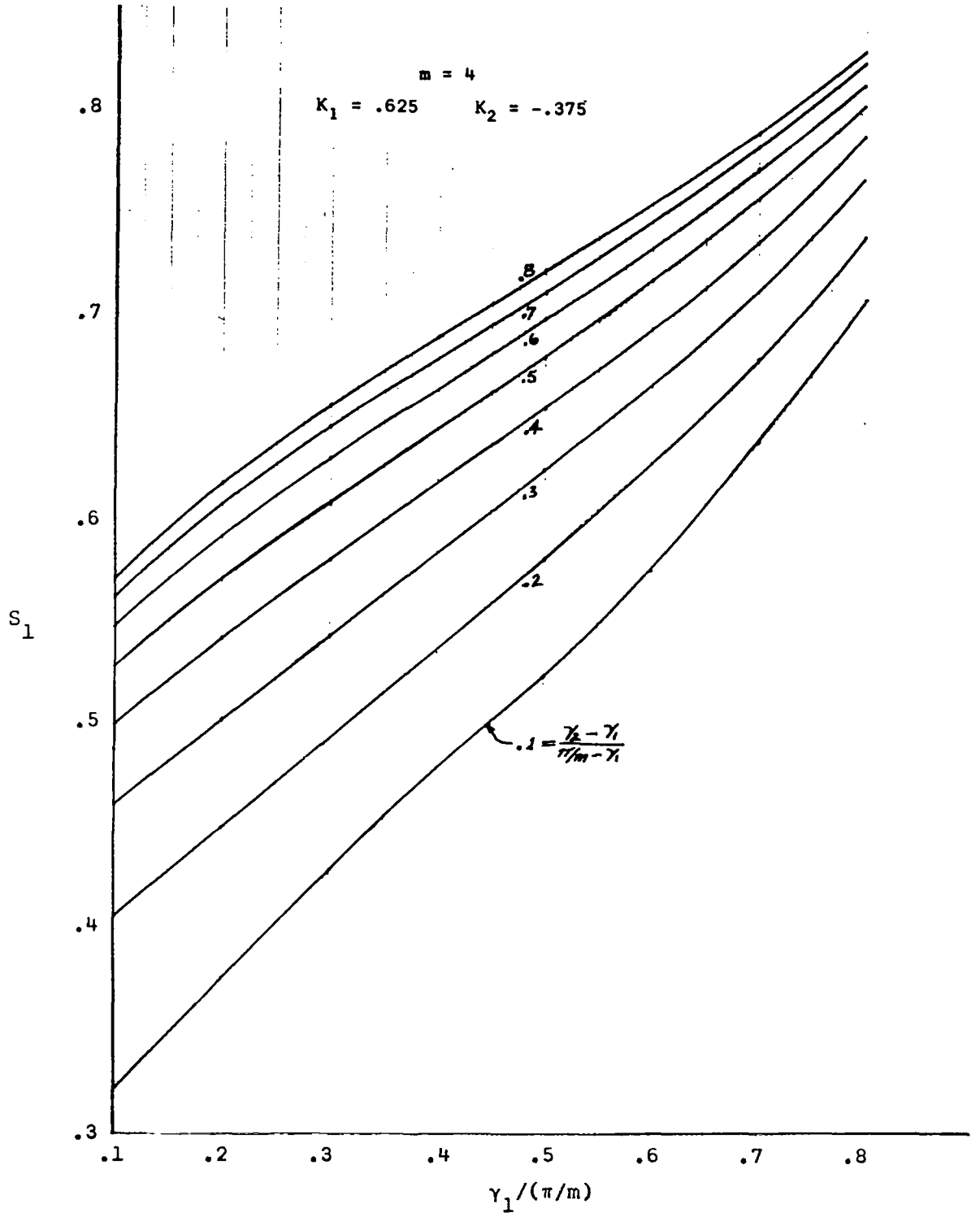

Figure S-3.- S_1 versus $\gamma_1/(\pi/m)$ for $(\gamma_2 - \gamma_1)/(\pi/m - \gamma_1)$ = constant.

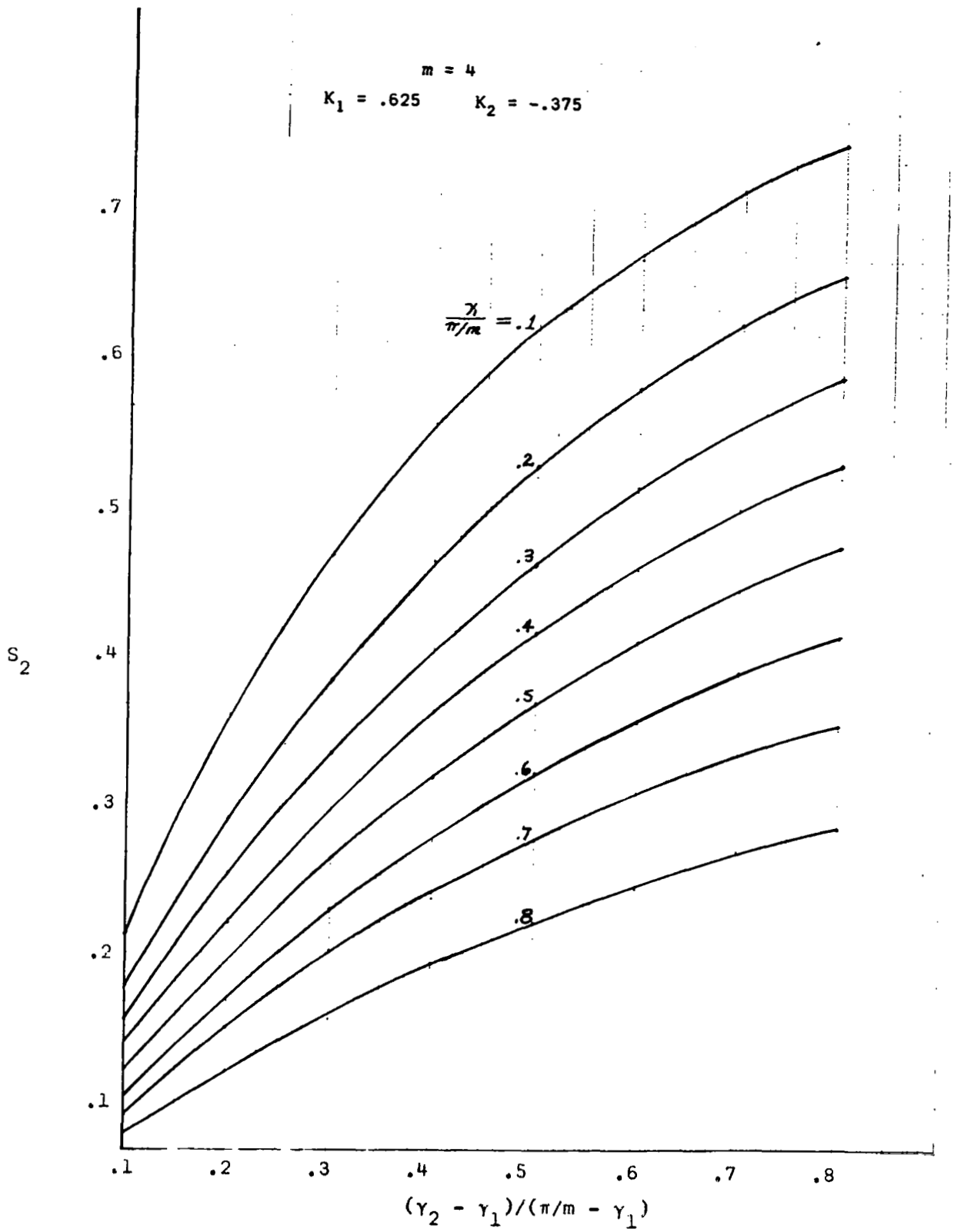

Figure S-4.- S_2 versus $(\gamma_2 - \gamma_1)/(\pi/m - \gamma_1)$ for $\gamma_1/(\pi/m)$ = constant.

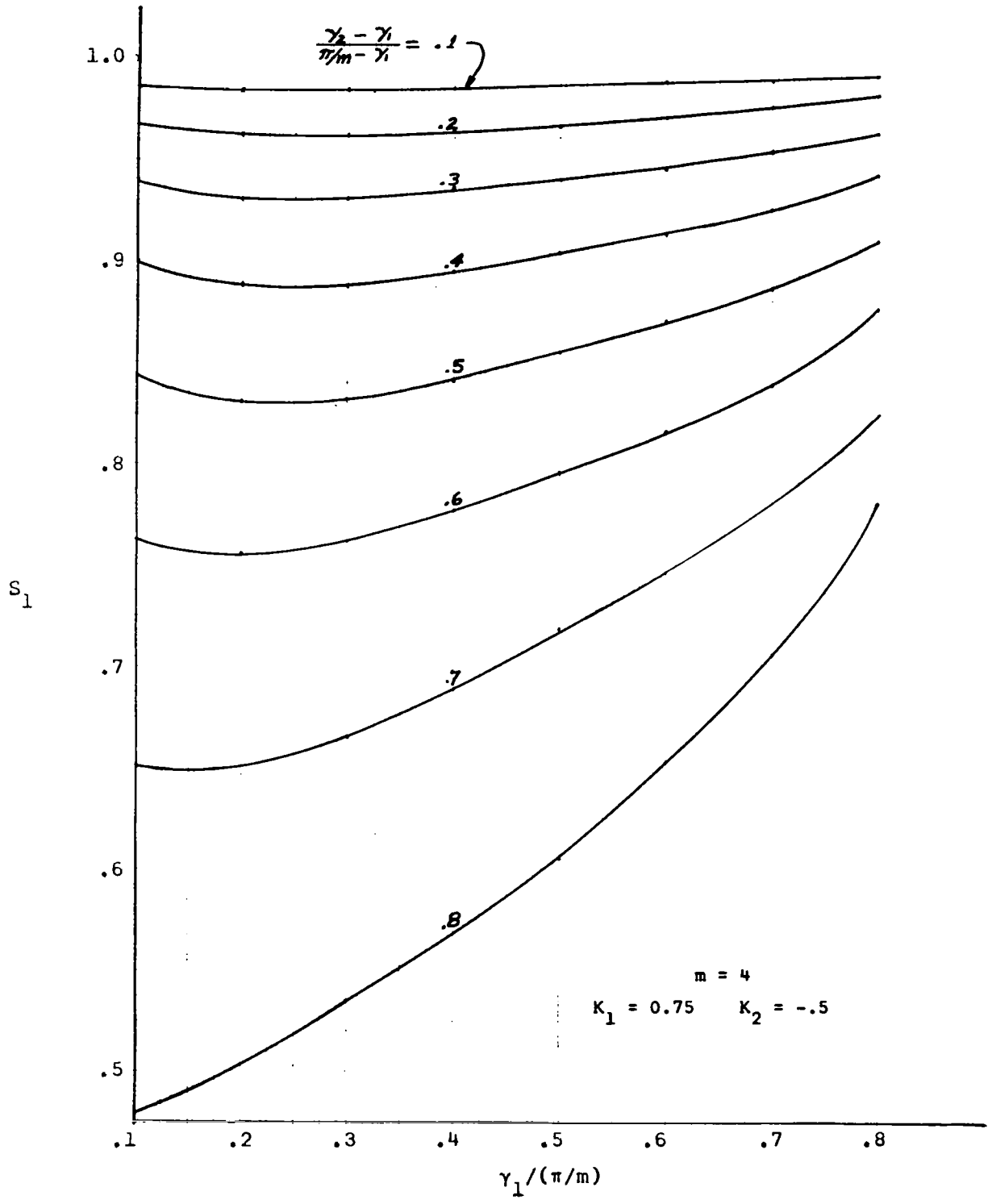

Figure S-5.- S_1 versus $\gamma_1/(\pi/m)$ for $(\gamma_2 - \gamma_1)/(\pi/m - \gamma_1)$ = constant.

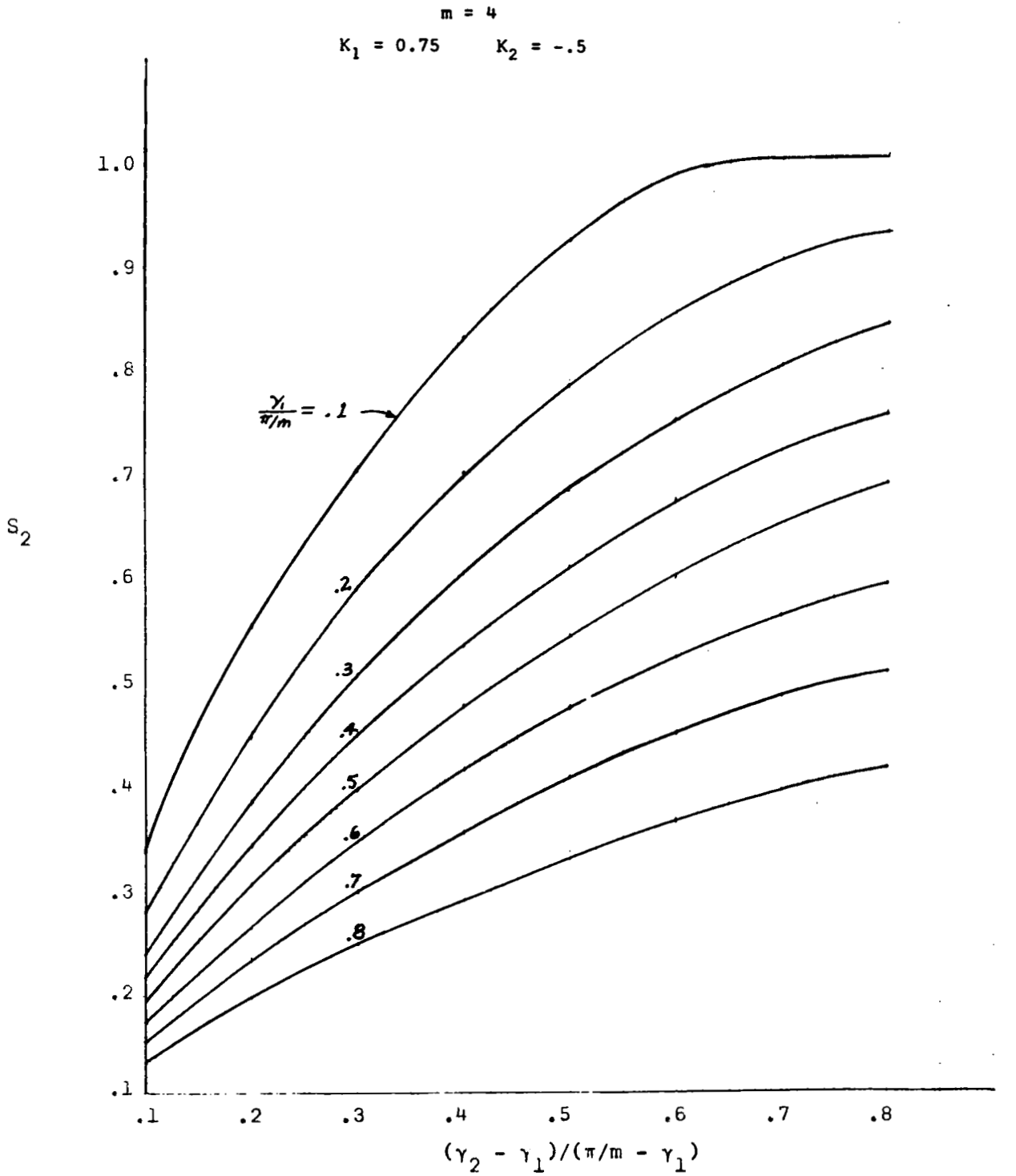

Figure S-6.- S_2 versus $(\gamma_2 - \gamma_1)/(\pi/m - \gamma_1)$ for $\gamma_1/(\pi/m)$ = constant.

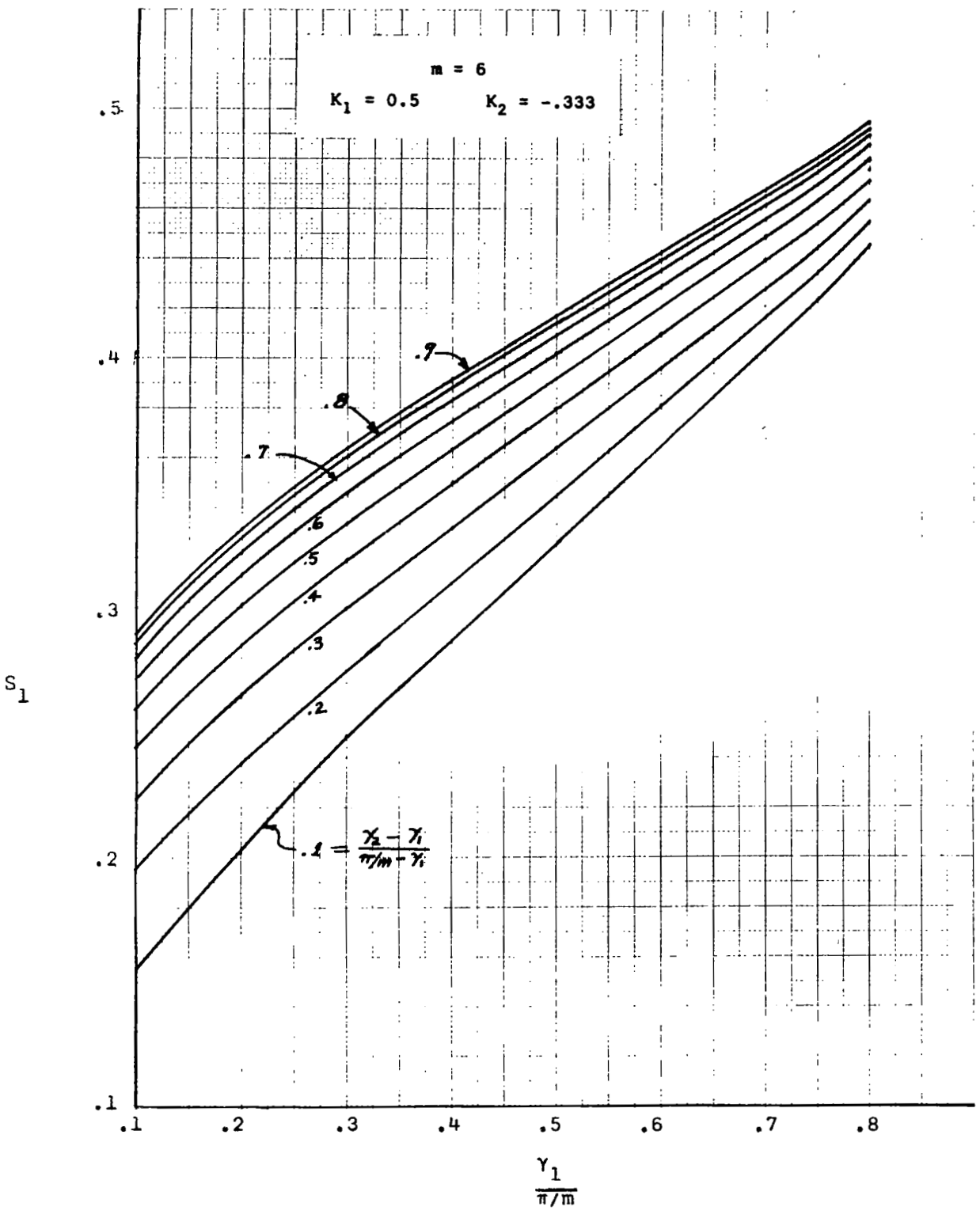

Figure S-7.- S_1 versus $\gamma_1/(\pi/m)$ for $(\gamma_2 - \gamma_1)/(\pi/m - \gamma_1)$ = constant.

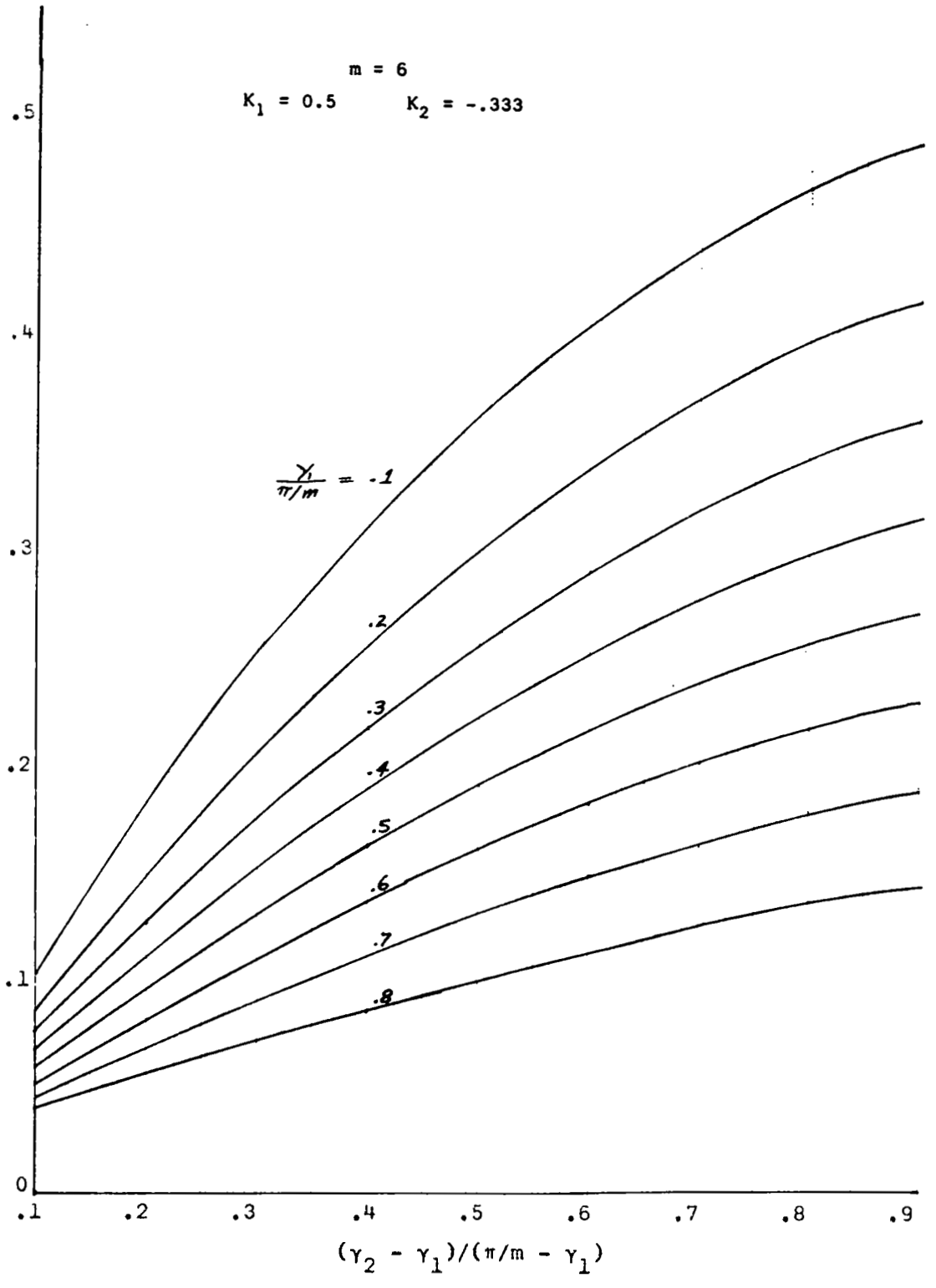

Figure S-8.- S_2 Versus $(\gamma_2 - \gamma_1)/(\pi/m - \gamma_1)$ for $\gamma_1/(\pi/m)$ = constant.

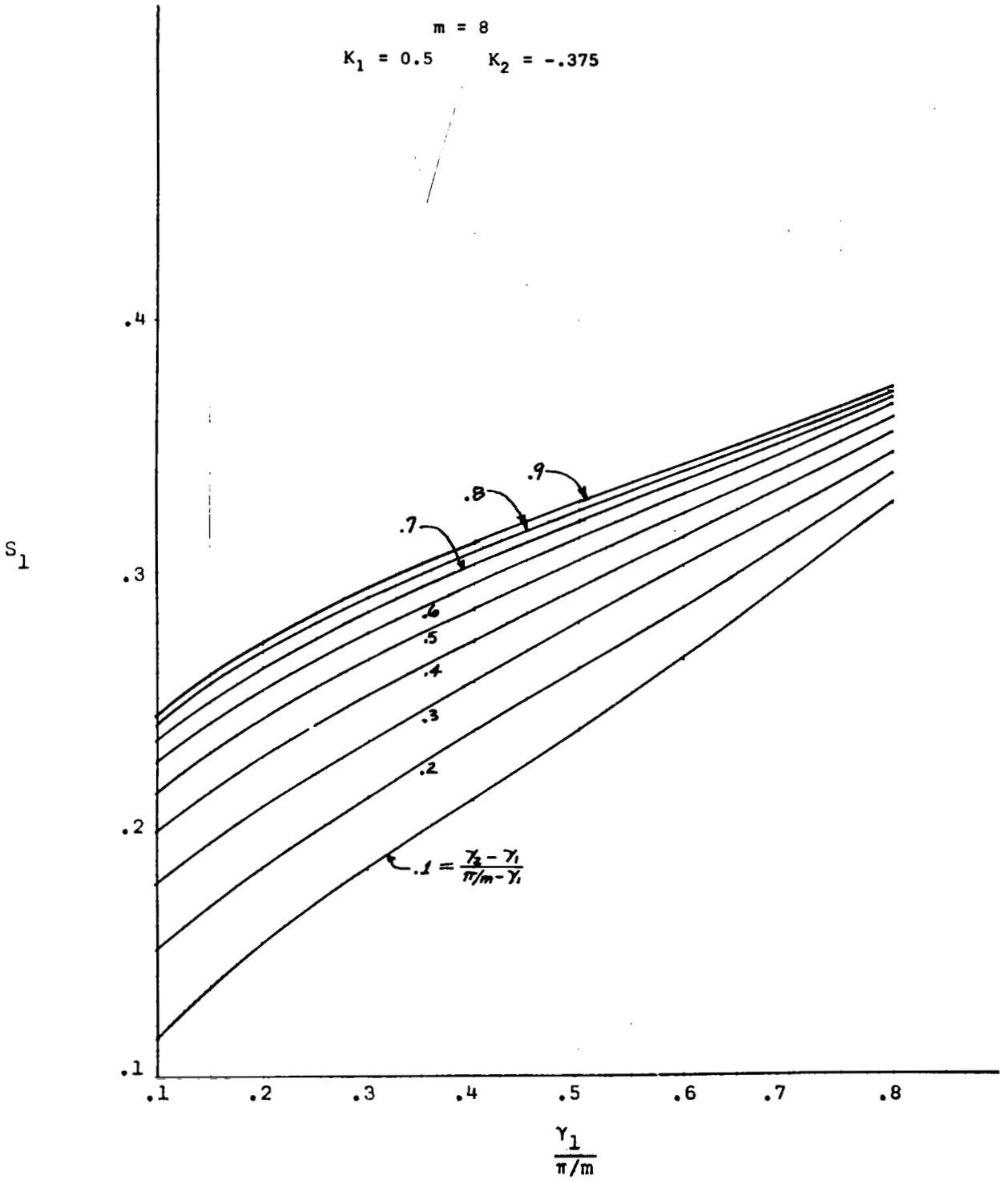

Figure S-9.- S_1 Versus $\gamma_1/(\pi/m)$ for $(\gamma_2 - \gamma_1)/(\pi/m - \gamma_1)$ = constant.

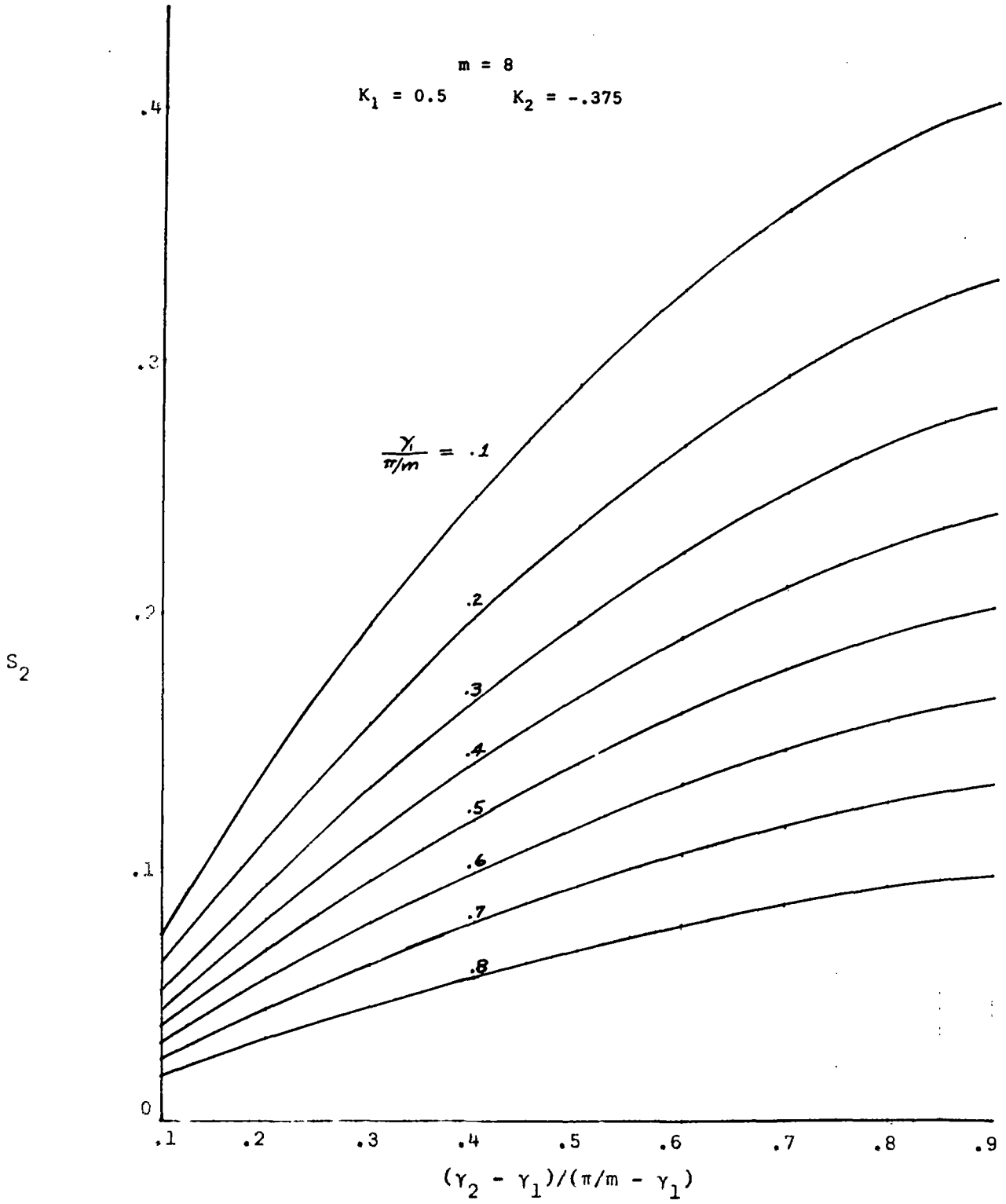

Figure S-10.- S_2 Versus $(\gamma_2 - \gamma_1)/(\pi/m - \gamma_1)$ for $\gamma_1/(\pi/m)$ = constant.

APPENDIX S-B. EXAMPLES OF VARIOUS STARS MAPPED BY EQUATION (S-5)

The following plots are included to illustrate the type and variety of maps which can be simply obtained from equation (S-5). Each example was constructed by following the algorithm presented in the section of "CONSTRUCTION OF MAPPING FUNCTIONS."

These plots were made on an IBM paper printer with a capacity of six characters per inch vertically and ten characters per inch horizontally. Thus each point (asterisk) may be in error by $\pm$ 1/12" vertically and $\pm$ 1/20" horizontally, making these plots somewhat crude in places. Hence these plots should not be used to examine the mapping near vertices, but they will give qualitative information on the degree of congruency of the map.

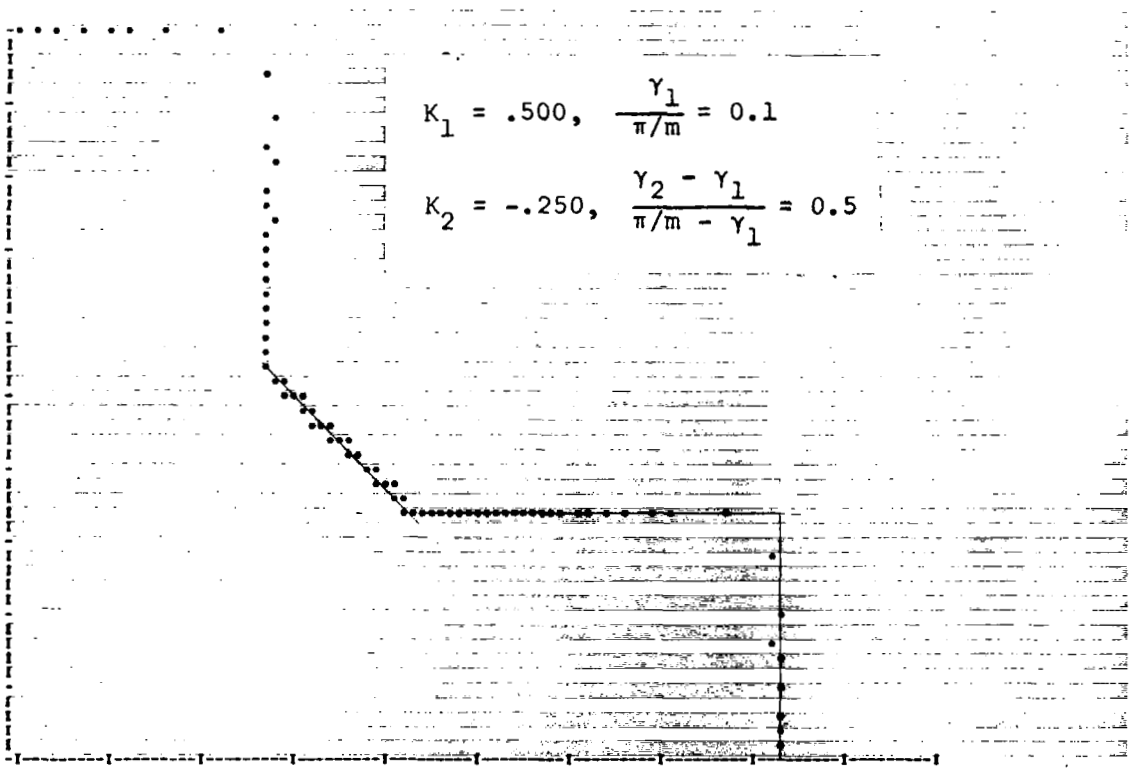

Figure S-11.- A 4-point second-degree star.

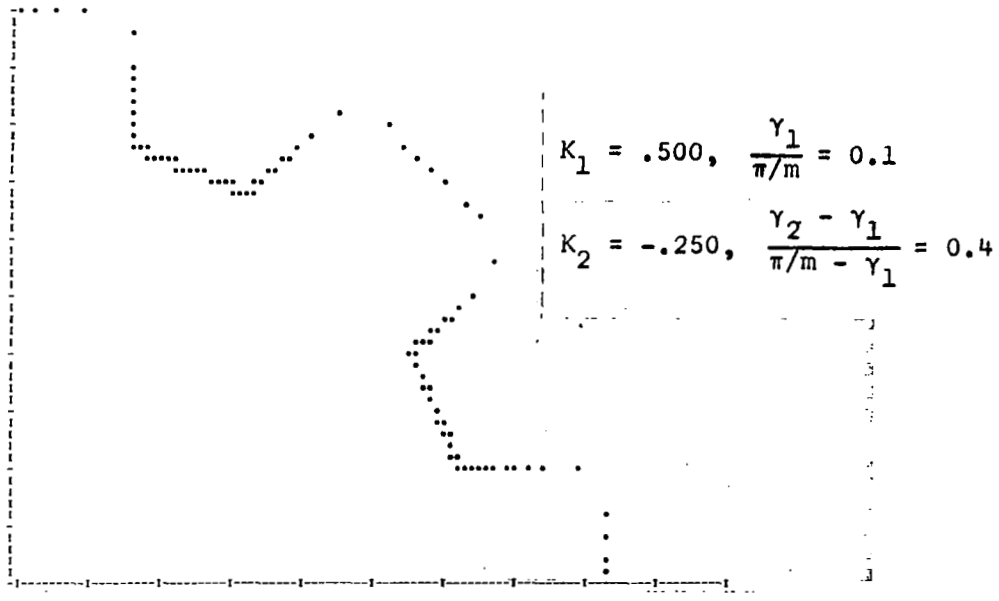

Figure S-12.- A 8-point second-degree star.

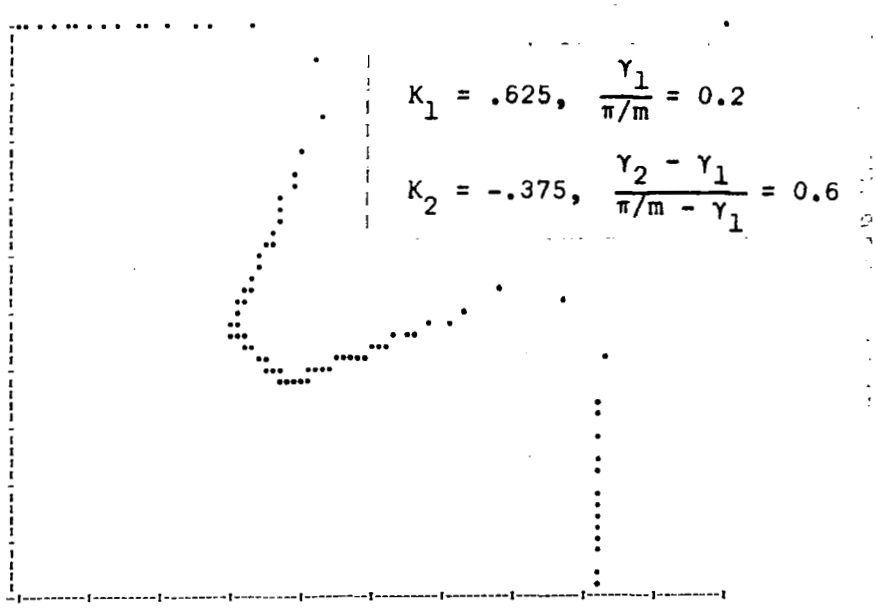

Figure S-13.- A 4-point second-degree star.

APPENDIX S-C. COMPUTER PROGRAMS

This Appendix is concerned with development of a polynomial mapping function on a digital computer. The programming has been broken down for clarity into a main or control program and a set of subprograms, each of which performs a calculation which corresponds to an equation in the text. These programs are written in FORTRAN IV for the IBM 7044. No attempt has been made to define input-output or plotting techniques as these are usually subject to rapid change and vary from installation to installation.

The control or main program essentially carries out the computations indicated by equations (4) through (7). Each subprogram accomplishes one logical block within that group. In all cases the symbolism used in the programs corresponds directly to that listed in the equations. Hence each subprogram is prefaced by only a brief explanation of its function.

INPUT DATA

SGN	Defines the type of mapping; -1 for exterior-to-exterior mapping, and +1 for interior-to-interior mapping.
M	The number of star points.
KK	The number of vertices required to define the shape of the star-shaped polygon.
AK(20)	Vector of vertex exterior angles (% of π).
GAMMA(20)	Vector of vertex image angles (% of π/m).
NC(20)	Vector which defines the order of polynomial desired at each vertex.

COMPUTED DATA

B(300)	An intermediate storage vector.
C(100)	Vector in which the polynomial coefficients for each vertex are generated.
D(300)	Vector containing the mapping function coefficients.
X & Y(300)	Vector containing the x and y coordinates of the star-shaped polygon produced by the mapping function.
NN	Number of terms minus one in the mapping function.
ALPHA	Normalizing coefficient.

FORTRAN PROGRAMS

1. Main Program:

This program is merely a device to pass control to the appropriate subprograms in the sequence required to generate and plot a mapping function.

```
      DIMENSIØN B(300), C(300), D(300), X(300), Y(300),
           AK(20), GAMMA(20), NC(20)
      READ (5,1) SGN, M, KK, ( AK(I), GAMMA(I), NC(I), I = 1, KK )
      NN = 1
      D(1) = 1.0
      AM = SGN*FLØAT(M)
      DØ 10 I = 1, KK
      AG = GAMMA(I)*3.1415927
      CALL PGEN ( C(1), NC(I), SGN, AK(I), M, AG )
      CALL PMUL ( D(1), NN, C(1), NC(I), B(1) )
      NN = NN + NC(I)
      DØ 10 J = 1, NN
   10 D(J) = B(J)
      NNP1 = NN + 1
      CALL PINT ( D(1), NNP1, 0.0, AM )
      CALL PNØRM ( D(1), NNP1, ALPHA, 1.0 )
C
C     The mapping function is now stored in vector  D.
C
      CALL PMAP ( D(1), NN, 1.0, AM, 1.0, 100, X(1), Y(1) )
      WRITE (6,2) ALPHA, ( D(I), I = 1, NNP1 ), ( X(I), Y(I), I = 1, 100 )
      END
```

2. Subprogram PGEN:

This subroutine generates the polynomial for each vertex; i.e., equation (4) or (S-4).

```
      SUBRØUTINE PGEN ( C, NC, SGN, AK, M, AG )
      DIMENSIØN C(300)
      AK1 = SGN*AK
      IF( AG .EQ. 0.0 .ØR. AG .GT. 3.1415 )  AK1 = AK1/2.0
      IND = NC + 1
      DØ 1 I = 1, IND
    1 C(I) = CSUM( I, AK1, M, AG )
      RETURN
      END
```

3. Subprogram CSUM:

This function-type subroutine generates the k-th coefficient $C_k(\gamma_j, K_j)$ defined by equation (4) or (S-4).

```
      FUNCTIØN CSUM ( I, AK1, M, AG )
      CSUM = 0.0
      KEND = (I+1)/2
      AN = I + 1
      M1 = I
      M2 = -1
      DØ 2 K = 1, KEND
      AN = AN - 2.0
```

```
      M1 = M1 - 1
      M2 = M2 + 1
      TERM = CØEF( AK1, M1 )*CØEF( AK1, M2 )
      IF( AN .NE. 0.0 )  TERM = 2.0*TERM*CØS(AN*AG)
    2 CSUM = CSUM + TERM
      IF ( I .EQ. (I/2)*2 ) CSUM = -CSUM
      RETURN
      END
```

4. Subprogram CØEF:

This function-type subroutine computes the factor $K(K - 1)(K - 2)\ldots(K - N)/\Gamma(N + 2)$ which is required in the calculation of coefficient C_k defined by equation (4) or (S-4).

```
      FUNCTIØN CØEF ( AK1, N )
      CØEF = 1.0
      IF ( N .EQ. 0 )  RETURN
      DØ 1 I = 1, N
      AN = I-1
    1 CØEF = CØEF*(AK1 - AN)/FLØAT (I)
      RETURN
      END
```

5. Subprogram PMUL:

This subroutine will multiply series A of order M by series B of order N. The result is stored in vector C (order M + N) and has M + N + 1 coefficients. This subroutine is used to accomplish the multiplication indicated by the integrand of equation (5).

```
      SUBRØUTINE PMUL ( A, M, B, N, C )
      DIMENSIØN A(300), B(300), C(300)
      NM = N+M
      C(1) = A(1)*B(1)
      DØ 20 I = 1, NM
      KP = 1
      IF(I .GT. N) KP = I+1-N
      KQ = I+1
      IF( KQ .GT. M ) KQ = M+1
      CC = 0.0
      DØ 18 J = KP, KQ
      KMI = I+2-J
   18 CC = CC+A(J)*B(KMI)
   20 C(I+1) = CC
      RETURN
      END
```

6. Subprogram PINT:

This subroutine evaluates the integral

$$\int_0^X \sum_{i=0}^{n} D_i X^{(A+i\cdot B)} dX.$$

This subroutine is used to accomplish the integration implied by equations (6) and (7), or (S-6) and (S-7).

```
      SUBRØUTINE  PINT ( D, N, A, B )
      DIMENSIØN D(300)
      DEN = C + 1.0 - D
      DØ 1 I = 1, N
      DEN = DEN + D
    1 D(I) = D(I)/DEN
      RETURN
      END
```

7. Subprogram PNØRM:

This subroutine will calculate and multiply a polynomial mapping function $z = f(\zeta)$ by a constant α such that at $\zeta = 1.0$ $z = BA$.

```
      SUBRØUTINE PNØRM ( D, N, ALPHA, BA )
      DIMENSIØN D(300)
      ALPHA = 0.0
      DØ 1 I = 1,N
    1 ALPHA = ALPHA + D(I)
      ALPHA = BA/ALPHA
      DØ 2 I = 1,N
    2 D(I) = D(I)*ALPHA
      RETURN
      END
```

8. Subprogram PMAP:

This subroutine will compute the x and y coordinates in the first quadrant of the star-shaped polygon (produced by the mapping function) at any $|\zeta|$. This subroutine is included because it eliminates all redundant sine and cosine calculations, which are usually a lengthy calculation on a digital computer.

$$z = A_0\zeta^C + A_1\zeta^{C+D} + A_2\zeta^{C+2D} + \ldots + A_n\zeta^{C+nD}$$

ζ = RØ*EXP(I*Ø); RØ = $|\zeta|$, I = $\sqrt{-1}$, Ø = Theta.

```
D       = The vector containing the mapping function coefficients.
NN      = The number of terms minus one in the mapping function.
NP      = The number of points to be plotted.
X & Y   = The vector where the points to be plotted are stored.

      SUBRØUTINE PMAP ( D, NN, C, D, RØ, NP, X, Y )
      DIMENSIØN D(300), X(300), Y(300)
      KP = NN+1
      JND = NP+1
      R = RØ**C
      RD = RØ**D
      DT = 1.5707963/FLØAT(NP)
      CCØ = 1.0
      SCØ = 0.0
      CDØ = 1.0
      SDØ = 0.0
      CCT = CØS(C*DT)
      SCT = SIN(C*DT)
      CDT = CØS(D*DT)
      SDT = SIN(D*DT)
      DØ 10 J = 1, JND
      RCD = R
      C1 = CCØ
      S1 = SCØ
      DD = A(1)*RCD
      BX = DD*CCØ
      BY = DD*SCØ
      DØ 5 I = 1, NN
      ST = S1*CDØ + C1*SDØ
      C1 = C1*CDØ - S1*SDØ
      S1 = ST
      RCD = RCD*RD
      DD = A(I+1)*RCD
      BX = BX + DD*C1
    5 BY = BY + DD*S1
      X(J) = BX
      Y(J) = BY
      ST = SCØ*CCT + CCØ*SCT
      CCØ = CCØ*CCT - SCØ*SCT
      SCØ = ST
      ST = SDØ*CDT + CDØ*SDT
      CDØ = CDØ*CDT - SDØ*SDT
   10 SDØ = ST
      RETURN
      END
```